Liquid penetration into a deformable porous substrate

K. S. A. Chen and L. E. Scriven

Researcher and professor, respectively, Coating Process Fundamentals Program, Dept. of Chemical Engineering & Materials Science, University of Minnesota, Minneapolis, Minn. 55455

ABSTRACT *In the coating of a porous substrate, the pore space is penetrated by liquid impelled (a) by hydrodynamic pressure that develops in the applicator and metering gaps and (b) by capillary pressure. Penetration is opposed by the pressure of any trapped air as it is compressed by invading liquid and the deformation of the substrate. From equations expressing the effects of these and associated factors, we can predict the performance of a combination roll applicator and metering blade for various dwell times. These predictions are computed and plotted to illustrate how contemporary methods of computer-aided analysis make practicable the modeling of so complicated a system. In exploring the effects of hydrodynamic pressure profile and dwell time, we found the degree of air-trapping within the substrate to be critical. The goal of models for blade coating is to be accurate enough for reliable troubleshooting, design, and optimization.*

KEYWORDS
Absorption
Analysis
Capillarity
Coating
Computer modeling
Dwell time

In coating, a layer of liquid or suspension is deposited on a substrate, and most of the air in contact with the substrate's surface is displaced. If the substrate is impermeable to air, the speed with which coating can take place is limited by undisplaced air. When the amount of undisplaced air becomes unacceptable, the situation is called "air entrainment."

When the substrate is porous and air entrained at the surface can "marry" that already in the pores, much higher speeds of acceptable coating can be attained before excessive entrainment, or skipping, occurs. But the situation is complicated by confinement and compression of air in the pore space as the coating liquid penetrates, particularly if the liquid wets the substrate. Air could be an important factor.

Here, we discuss the physics of liquid penetration into a porous substrate like paper. We also discuss the displacement of air in the pore space.

Background

Many studies of liquid penetration have been reported in published work. The effect of air in the pore space previously had not been considered when our work was in progress; however, it has been recognized independently by Eklund and Salminen (*1*) following Saita and Scriven (*2*).

Confinement and compression are most severe when the substrate is pressed so hard against a backup roll or other supporting surface that air has no egress and is trapped. At the opposite extreme is the absence of confinement and compression. Those are the situations considered here.

The coating configuration studied consists of a roll applicator and a bevelled blade metering element, the two separated by a variable distance, and thus a variable dwell time (**Fig. 1**). The conditions at the bevelled blade are those of the base case in the companion paper on the physics of flexible blade coating of an elastic substrate (*3*). Consideration is limited to steady states that are two-dimensional (no variation across the substrate). Both studies were aimed at advancing the understanding of paper coating processes in terms of basic principles. They follow two earlier contributions (*2, 4*).

In blade coating, the effects of liquid penetration, or dewatering, on coating weight and quality and process "runnability" have been studied extensively (*1, 5–12*). Evidently, one result is the evolution of technology from flooded-nip blade coaters to short-dwell-time design to variable-dwell-time configurations that afford some control over the extent of liquid penetration into the substrate.

How this control comes about was

first addressed by Eklund and Salminen (*1, 9*). They modified a Lucas-Washburn equation to account for (a) forced penetration of liquid driven by external hydrodynamic pressure and (b) spontaneous penetration driven by capillary pressure induced by wetting. They also rationalized the evidence of a short delay time in the spontaneous penetration by suggesting that strong wetting develops only after surface modification by absorption. They approximated the hydrodynamic pressure as constant in the zones of elevated pressure. (Far from being constant, this hydrodynamic pressure rises from atmospheric pressure upstream, peaks near the minimum gap, falls to subambient pressure, and recovers to atmospheric pressure downstream.) They concluded that the influence of dwell time is considerably less than that of hydrodynamic pressure but that, at longer dwell times, the penetration depth ought nonetheless to approach proportionality with the square root of dwell time, as in their modified Lucas-Washburn equation.

This expectation was not born out by the results of the experiments with an apparatus akin to a Bristow wheel (*1, 9, 10*). They pointed out that complicating factors not taken into account include the counter-pressure of air in the pore space, the absorption of liquid into the fibers of the matrix, and the accompanying swelling of the fibers. To these can be added the variation of hydrodynamic pressure along the substrate surface and the compression of the substrate. Such compression is accompanied by changes in porosity, permeability, and depth of penetration. Several of the concepts advocated by Eklund and Salminen are central in our present paper.

That air is compressed in the forced penetration of liquid into paper backed by a smooth or deformable surface and that it can subsequently re-expand was recently incorporated into a rudimentary model of water sorption at short times by Eklund and Salminen (*1*). Though the model misses the variation of hydrodynamic pressure along the substrate surface in a coating operation, the conclusions they draw appear to accord qualitatively with the findings reported here.

The only attempt at systematic analysis of effects of substrate compressibility appears to be that of Tayler (*13*), who took the local compression of paper to be proportional to the local difference between hydrodynamic pressure on the surface and atmospheric pressure. This model is employed here. It can readily be extended to account for nonlinear dependence of paper thickness on the applied hydrodynamic pressure and on internal pore pressure.

1. Schematic of a flooded nip blade coating process. To the right is the take-away zone (not shown).

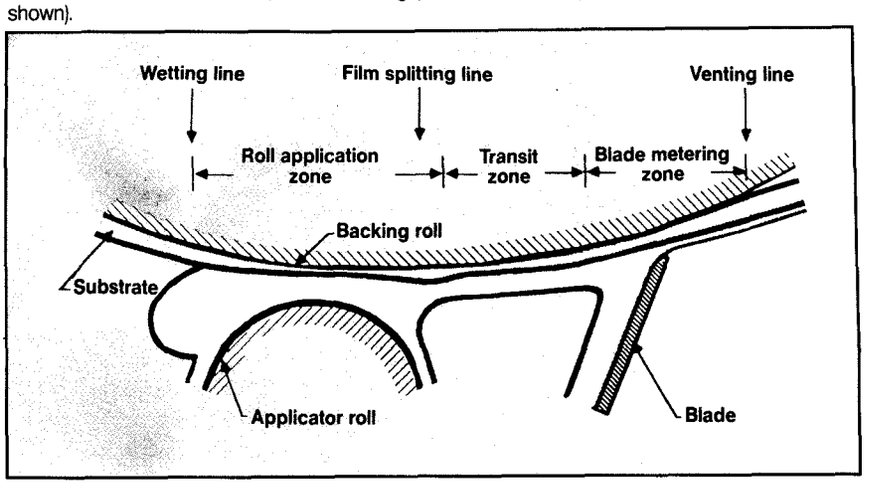

Principles and approximations

Liquid flow

Flow in porous material is governed by Darcy's law. Locally, the volumetric flux per unit cross-section q is proportional to the negative of the mechanical potential gradient, of which only the pressure gradient ∇p is relevant here, and is inversely proportional to the liquid's viscosity, μ. The proportionality constant is the permeability of the material to the liquid, k.

The permeability k is an average or macroscopic property. It depends on local sizes, shapes, and how well the pores are connected. The pore structure is highly irregular in paper as in most porous media. Except when liquid completely fills the pore space, the paper's permeability to liquid also depends on the way liquid is distributed locally. If wetting is spontaneous, arising from capillary forces, the liquid invades preferentially along surfaces and through small passages (i.e., sequences of segments consisting of constrictions and adjacent enlargements). Some of the originally resident gas may be surrounded by liquid and be trapped in pore enlargements (*14*).

If wetting is coerced by external pressures, the liquid invades mainly through larger passages, so that some of the gas, instead of being displaced, is trapped in smaller passages (*15*). To our knowledge, no one has studied how liquids and suspensions trap air as they penetrate paper, so we adopted a simplifying approximation: that the invading liquid totally displaces the resident air all along a sharply defined front. Only the permeability of the filled pore space behind that front is relevant. In these circumstances, the appropriate form of Darcy's law is (*16, 17*):

$$q = -(k/\mu)\,\nabla p \qquad (1A)$$

The pressure gradient almost is perpendicular to the surface of the porous material where liquid invades; that is, it can be approximated as lying exactly in the z direction. Thus, the form of Darcy's law actually employed here is

$$q(x,z) = -\frac{k(x,z)}{\mu}\,\frac{dp}{dz} \qquad (1B)$$

In deformable porous media undergoing compression or expansion, the sizes and shapes of pore segments may change. Indeed, the constrictions in pore segments may be occluded, or occluded ones may be opened, so that the connectivity of pore space changes. As a simplifying approximation, the local permeability to liquid, k, is regarded as being isotropic and depending solely on local porosity ϕ.

A qualitatively reasonable functional form comes from the Kozeny-Carman relation. Originally put forward for materials that are assemblages of granules, this relation has proved somewhat more widely applicable (*18*):

$$\frac{k(\phi)}{k_o} = \left[\frac{\phi}{\phi_o}\right]^3 \left[\frac{1-\phi_o}{1-\phi}\right]^2 \quad (2)$$

The term k_0 is the permeability in the uncompressed state. The quantities k and k_0 are measured in units of H_0^2, H_0 being the undeformed thickness of the substrate.

Substrate compression

Supported on one side by solid and exposed on the other to liquid under pressure, a porous material deforms. The amount of deformation depends on not only the rigidity of the solid matrix, but also the pressure of the fluid in the pore space (*19*). When liquid is invading, that pressure varies with depth, so the compression is not uniform. For simplicity, however, the pressure is regarded here as uniform at any given distance x along the surface. To simplify further, the difference between thickness H_0 at atmospheric pressure and local thickness $H(x)$ under loading by liquid at pressure $p(x)$ is taken as linear in the pressure difference (*3*, *13*). With thicknesses measured in units of H_0 and pressures in units of $\mu U_w/H_0$, the relation is

$$1 - H(x) = \left[\frac{\mu U_w}{EH^2}\right][p(x - p_a)] \quad (3)$$

E is the z-direction modulus under the type of loading and support, or backup roll, just described.

Provided the density of the solid matrix does not change appreciably with pressure or other factors (such as swelling, which is not considered here), simple geometry gives the relationship between porosity and compression:

$$\phi(x) = 1 - \frac{1-\phi_o}{H(x)} \quad (4)$$

ϕ is the porosity at atmospheric pressure. Equations 1-4 are elements of a model of liquid penetration, but more are needed.

Liquid penetration

Suppose at distance x (measured in units of H_0) along the porous substrate, the liquid has penetrated to depth $Z(x)$ (in units of H_0). The form of Darcy's law in Eq. 1B can be integrated to that depth to give a relationship between penetration rate $v(x) \equiv q(x,0)$ (measured in units of U_w) and the difference between liquid pressure at the substrate surface $[p(x,0)]$ and the pressure right behind the liquid front within the pore space $[p(x,Z(x))]$:

$$v(x) = k(x)\ \frac{p(x,0) - p(x,Z(x))}{Z(x)} \quad (5)$$

According to the Young-Laplace equation of capillarity (*14*, *16*, *17*), the pressure behind the liquid front within the pore space is the sum of the gas (air) pressure, $p_G(x)$, just ahead of the front and the capillary pressure, $-p_c$, across the front:

$$p(x,Z(x)) = p_G(x) - p_c \quad (6A)$$

The capillary pressure is actually a pressure difference. It is the resultant of surface tension σ when the interface is curved: $(\mu U_w/\sigma)p_c = 2/r$, where r, measured in units of H_0, is a certain mean radius of curvature of the interfaces at the front. This curvature can depend on the apparent contact angle with matrix surface, which locally may be zero or nearly so (*14*, *20*). In spontaneous imbibition through capillary action, these interfaces are concave toward the air ahead of the front, and r is positive. The interfaces are made concave toward the air because they merge into thinfilms of wetting liquid ahead of the front; locally, the apparent contact angle with matrix surface is zero or nearly so (*19*, *20*).

In penetration primarily forced by pressure, thin-films have insufficient time to develop even if the solid matrix is covered by precursor films. Instead, the interfaces are made convex toward the air by the liquid's more ready advance in the centers of pores. In this circumstance, however, the capillary pressure is likely to be small compared to the impressed pressure difference $p(x,0) - p_G(x)$. So as a simplifying approximation, the capillary pressure p_c is here taken as constant and equal to the spontaneous imbibition value. (If there were any cylindrical pore segments, the mean radius would be $r \cos\theta$, r being the cylinder radius in units of H_0 and θ the apparent contact angle of the interface with the cylinder. Generally, the chance of any cylindrical pore segments being present in paper is nil.)

The penetration rate, according to Eqs. 5 and 6A, is, with $p(x,0)$ written as $p(x)$ for simplicity:

$$v(x) = k(x)\ \frac{p(x) - p_G(x) + p_c}{Z(x)} \quad (6B)$$

This must equal the rate of change of liquid inventory in the pore space. With velocities measured in units of substrate speed U_w, time in units of H_0/U_w, and distance x in units of H_0, so that $dx/dt = 1$, this means:

$$v(x) = \frac{d(\phi Z)}{dt} = \frac{d(\phi Z)}{dx}\frac{dx}{dt} = \frac{d[\phi(x)Z(x)]}{dx} \quad (7)$$

(If $p(x) = p_G(x)$ and k and ϕ were all constant, combining Eqs. 6B and 7 and integrating would yield $Z = (2k\,p_c t)^{1/2}$, which makes plain how the old Lucas-Washburn formula, which though incorrect has the appropriate functional form (*17*), has to be interpreted in terms of the physics of liquid penetration into porous media. Note that here Z is measured in units of H_0, k is in units of H_0^2, p_c is in units of $\mu U_w/H_0$, and t is in units of H_0/U_w.)

Air compression

Beneath the liquid-filled part of the porous material is the air-laden part, as indicated in the enlargement in **Fig. 2**. The flow of the air also is described by Darcy's law. The volumetric flux caused by the same pressure gradient is larger than that of liquid by a factor that is the ratio of liquid viscosity to gas viscosity. The escape of air from the lateral edges of a wide sheet is negligible, but there may be appreciable movement in the machine direction within the pore space. The governing equations are straightforward.

The principle of conservation of the mass of air requires that $dm/dx = 0$. The down-web coordinate x is measured in units of H_0. The mass flux m, measured in units of $\rho_a U_w H_0$ (ρ_a being air density at ambient conditions), is

$$m = \frac{\rho_G}{\rho_a}\left[\phi - \left(\frac{\mu}{\mu_G}k\right)\frac{dp_G}{dx}\right](H - Z) \quad (8)$$

The first term represents convection of air with the velocity of the porous material; the second represents the Darcy flow relative to that convection. Here ρ_G is the local air density, μ_G is its viscosity, and p_G is its pressure (with the pressure measured in units of $\mu U_w/H_0$).

The air can be treated as a perfect gas. Its compression can be treated as polytropic—that is, $p_G V_G^n$ = constant, where n is the polytropic exponent:

$$\frac{\rho_G(x)}{\rho_a} = \left[\frac{p_G(x)}{p_a}\right]^{1/n} \quad (9)$$

Equations 8 and 9, together with $dm/dx = 0$, yield the equation that governs air flow along the porous material:

$$\frac{d}{dx}\left\{\left[\frac{p_G(x)}{p_a}\right]^{1/n}[H(x) - Z(x)]\left[\phi(x) - k_G\frac{dp_G}{dx}\right]\right\} = 0 \quad (10)$$

where $k_G = (\mu/\mu_G)k$. This second-order differential equation calls for boundary conditions upstream at the dynamic wetting line region ($x = x_0$) and downstream at the venting line region ($x = x_v$). General conditions are that at both boundaries the Darcy flux is proportional to the local gauge pressure just inside the porous material:

$$k_g\frac{dp_G}{dx} = \alpha(p_G - p_a) \text{ at } x = x_o$$

$$k_g\frac{dp_G}{dx} = \beta(p_G - p_a) \text{ at } x = x_v \quad (11)$$

The "air transfer coefficients" α and β characterize the air flow just outside and just inside the dynamic wetting line and the venting line, respectively. They can be estimated from more refined analysis, and they could in principle be estimated from suitable experimental measurements. However, there are two limiting cases, and these define the boundaries of the effect of air movement in the pore space.

In the first limit $\alpha(x_v - x_0)/k_G \to 0$ and so air is able to flow and escape as fast as any pressure gradient could develop.

2. Defining sketches of the roll application zone, with wetting line and film split, showing an enlargement of flow in the porous substrate with the penetration front

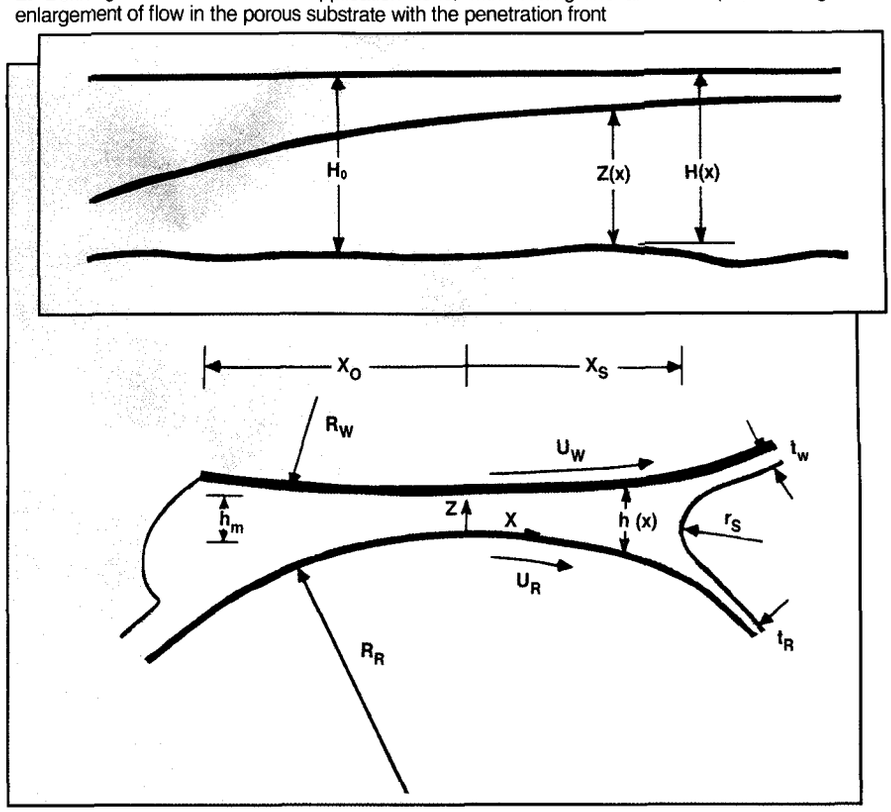

Then, there is no air trapping, and Eqs. 10 and 11 reduce to Eq. 12:

$$p_G = p_a \quad (12)$$

This extreme case is considered below. In the second limit, $k_G/\alpha\ (x_v - x_0) \to 0$ In this case, air is unable to flow: once liquid begins to penetrate, the front along which it displaces air is so sharp that all of the air initially present at atmospheric pressure is trapped at its initial location in the pore space. There it remains until that location reaches the place downstream where the underside of the sheet lifts off the backup roll, thereby venting the trapped air to atmospheric pressure. In this limit of complete air trapping, Eqs. 10 and 11 reduce to

$$\frac{p_G(x)}{p_a} = \left\{\frac{\phi_o}{[H(x) - Z(x)\ \phi(x)]}\right\}^n \quad (13)$$

Liquid penetration into an air-laden, deformable porous substrate is described, within the simplifying approximations recounted above, by Eqs. 2-7 and either Eqs. 10-11 or Eqs. 12 or 13. Here, we will consider further only the two limiting cases. In both, there are seven independent equations that interrelate eight unknown functions of distance x along the substrate from the place where penetration begins.

An additional equation is needed. It is the equation for the pressure distribution $p(x)$ in the liquid external to the porous medium. This equation involves additional unknown functions and brings additional equations into the completed model. [The varying pressure in the external liquid is absent from the model of Eklund and Salminen (*1*).]

External flow region

For our purposes here, the complete external flow region can be divided in four zones: the application zone, the variable length transit zone, the metering zone, and the terminal transit or take-away zone. All but the last are shown in Fig. 1.

Application zone

The applicator considered is a forward roll coater, as shown in Fig. 2. Key features are the film split on the

downstream side of the nip and the wetting line at which liquid starts penetrating the substrate upstream of the nip. Flow between these two locations is nearly rectilinear and is fairly well described by the lubrication approximation (*4, 21, 22*). Here, the lubrication approximation is extended to compressible porous substrate.

The mean surface speed of the coating roll and of the web or substrate when all speeds are measured in units of U_w is $U \equiv (U_R + 1)/2$. The effective radius R of the coating roll and substrate wrapping the backing roll is given by $2R^{-1} = R_w^{-1} + R_R^{-1}$ with all the radii being measured in units of H_0 (*23*). (When R_w is much larger than R_R, as in many practical situations, $R = 2R_R$). An excellent approximation to the local clearance $h(x)$ (in units of H_0) between the two surfaces is

$$h(x) = \frac{h_m}{H_o} + \frac{x^2}{R} + [1 - H(x)] \qquad (14)$$

Here, H_0 is the minimum clearance when the substrate is not compressed (i.e., when its thickness is H_0) and x is the distance from the minimum clearance, or nip (in units of H_0).

According to Reynolds' lubrication approximation (*23*), the volumetric flux $Q(x)$, measured in units of U_wH_0, is the sum of plug flow and Poiseuille flow contributions (with pressure always measured in units of $\mu\ U_w/H_0$):

$$Q(x) = Uh(x) - \frac{[h(x)]^3}{12}\frac{dp}{dx} \qquad (15)$$

Conservation of mass requires that volumetric flux $Q(x)$ in the clearance diminish as liquid leaves to penetrate the porous substrate:

$$dQ/dx = -v(x) \qquad (16)$$

Now, for the ten functions, the ninth and tenth being h(x) and Q(x), there are ten independent equations, Eqs. 2-7, 12 or 13, and 14-16. But Eqs. 7, 15, and 16 are differential equations, and boundary conditions are needed.

The upstream boundary is the wetting line. There, the liquid pressure is atmospheric, and there is no liquid in the pore space. A fair approximation is to put the wetting line one-sixth of an effective radius upstream. Thus

$$p = p_a,\ Z = 0 \text{ at } x = x_0 = -R/6 \qquad (17)$$

The downstream boundary of the application zone is the stagnation line at which the film splits. Its location is an unknown, x_s, which brings additional equations and unknowns (*4, 21, 22*). The pressure balance at the film split is

$$p(x_s) - p_a = -\left[\frac{\sigma}{\mu U_W}\right]\frac{1}{r_s} \qquad (18)$$

where r_s, a function of x_s, is the radius of curvature of the splitting film,

$$r_s = \frac{1}{2}\left[h(x_s) - t_R - t_w\right] \qquad (19)$$

where $h(x_s)$ is the clearance at x_s, and t_R, also a function of x_s, is the final thickness of the layer carried away on the roll:

$$t_R = h(x_s)\sqrt{U_R}/3(1 + \sqrt{U_R}) \qquad (20)$$

and $t_w = t_w(x_s + r_s)$ is the thickness of the layer carried away on the substrate at $x = x_s + r_s$, where the velocity throughout the layer is virtually that of the substrate:

$$t_w(x_s + r_s) = h(x_s)/3(1 + \sqrt{U_R}) \qquad (21)$$

The total flux carried away from the split is (apart from a trace of exchange with the substrate)

$$Q = U_R t_R + t_w(x_s + r_s) \qquad (22)$$

This value must be equal to the total flux arriving at the film split, as given by Eq. 15:

$$Q = Uh - \frac{h^3}{12}\frac{dp}{dx} \quad \text{at } x = x_s \qquad (23)$$

Moreover, $h(x_s)$ must be as required by Eq. 14:

$$h(x_s) = \frac{h_m}{H_0} + \frac{x_s^2}{R} + [1 - H(x_s)] \qquad (24)$$

With this, the model of the application zone is complete. The parameters of the model are as given in **Table I.** How these equations were solved is described elsewhere (*24*).

Transit zone

The transit zone is the variable distance L (measured in units of H_0) between (a) the place ($x = x_s + r_s$) just downstream of the film-split, where the liquid layer on the substrate, or web, has thickness t_w ($x_s + r_s$) and (b) the place ($x = x_s + r_s + L$) just upstream of the metering blade, which is chosen as the inflow plane of that zone. Over this distance, the pressure in the liquid layer is atmospheric. The air trapped and compressed within the substrate by the liquid that has penetrated tends to expand, expelling some of the liquid. Moreover, the substrate is in its uncompressed state.

As Eqs. 5 and 6 confirm, if the distance L were great enough, the air would expand until it reached equilibrium at $p_G = p_a + p_c$. According to Eq. 13, the corresponding penetration (in units of H_0) would be $Z_{eq} = 1 - (1 + p_c/p_a)^{-1/n}$. The rate of approach toward this limit is controlled by permeability and viscosity and is governed by Eqs. 5-7, 13, and 16, with $\phi(x) = \phi_0$, $H(x) = 1$, $Q(x) = t_w(x)$ (in units of H_0), and initial conditions $t_w(x_s + r_s) = t_w$ and $Z(x_s + r_s) = \phi(x_s)Z(x_s)/\phi_0$. Because they are a subset of those that govern the application zone, these equations were conveniently solved simultaneously with those others and in the same way. The outputs were the layer thickness t_w ($x_s + r_s + L$) and the liquid penetration depth $Z(x_s + r_s + L)$ at the inflow plane of the metering zone.

Metering zone

The metering element is a bevelled blade (*3*). For simplicity, the blade's elasticity is set aside, and a fixed blade configuration is adopted which is exactly that of the base case (*3*). The only other difference is that besides no slip at the substrate surface, liquid may enter or leave the substrate:

$$v_x = 1 \quad \text{at } z = H(x) \qquad (25)$$

$$v_z = v(x) \text{ at } z = H(x) \qquad (26)$$

Moreover, the inventory ϕZ within the substrate at the start of the metering zone ($x = x_s + r_s + L$) is what arrives at the end of the transit zone.

In the metering zone, as in the application zone, the penetration process is described by Eqs. 2-7, and 12 or 13. An added boundary condition is that at the outflow plane of the metering zone, the underside of the substrate lifts off the backup roll, venting to the atmosphere the gas trapped within the substrate. The equations of the metering zone model Eqs. 2-7, 12 or 13, 25, 26, and 1-7 of the companion paper (*3*) also were

solved by a Galerkin/finite element method (*24*). (All lengths were measured in units of H_0, the thickness of the uncompressed substrate sheet; in the companion paper, it is arbitrary but was also taken as 0.1 mm.)

Take-away zone

Downstream of the venting line that terminates the metering zone is a second transit zone. In this zone, no air is trapped, and capillary pressure is unopposed. Thus, capillary pressure can draw in liquid from the layer that coats the substrate surface, until the layer is gone or until all the pore space is filled. Ordinarily, coating processes (in contrast with some impregnation processes) are so controlled that the thickness $t_w(x_v)$ of the layer that at first remains on the surface is far less than would fill all the pore space. Then the equilibrium state approached downstream is penetration to the depth $Z(x_v) + t_w(x_v)/\phi_0$.

Estimation of overall penetration

In the final coated state, the substrate is undeformed, according to the model. Consequently, the effect on porosity of the temporary deformations in the application and metering zone is inconsequential, and Eqs. 5 and 7 can be combined and formally integrated from the wetting line to just short of the venting line to give (with pressures measured in units of $\mu U_w/H_0$, etc.):

$$\frac{[Z(x_v)]^2}{2k} = \int_{x_0}^{x_v} [p(x') - p_G(x')]\, dx' + [x_v - x_0]\, p_c \qquad (27)$$

The last term on the right corresponds to spontaneous penetration by capillary pressure alone—as given by formulas of Lucas-Washburn type. The first term on the right corresponds to forced penetration driven by external pressure and opposed by the pressure of trapped air as it is compressed. Apart from the viscous resistance to liquid flow in response to the pressure difference, the air pressure p_G is controlled by the hydrodynamic pressure p. Consequently, the net effect of forced penetration in the application and metering zones would be nil if the trapped air were allowed to re-expand to atmospheric pressure

I. Parameters for the application zone model

Uncompressed porosity ϕ_0	0.5
Uncompressed permeability k_0 (in units of H_0^2)	3.7×10^{-6}
Ratio of minimum clearance to uncompressed thickness h_m/H_0	4
Compressibility number ($N_{Co} \equiv \mu U_w/EH_0^2$)	1×10^{-4}
Capillary pressure p_c (in units of U_w/H_0)	0.95
Capillary number $N_{Ca} \equiv \mu U_w/\sigma$	15
Roll speed ratio, i.e. U_R measured in units of U_W	0.2
Ratio of effective roll radius to substrate thickness (i.e. R measured in units of H_0)	4×10^3
Polytropic air compression exponent n	1.4

II. Parameter values in the extended base case

	Dimensional	*Dimensionless*
Substrate thickness, H_0	100 μm	1
Substrate speed	15 m/s	1
Applicator roll radius	20 cm	2×10^3
Applicator roll speed	3 m/s	0.2
Applicator-to-backing roll gap	500 μm	5
Dwell distance in transit zone	7.5 cm	750
Blade thickness	0.206 mm	2.06
Blade working angle (fixed)	51°	...
Blade bevel angle	135°	...
Blade-to-backing roll gap	114 μm	1.14
Viscosity of liquid	50 mPa · s	...
Surface tension of liquid	50 mN/m	...
Density of liquid	1200 kg/m^3	...
Capillary pressure of liquid in substrate	0.07 atm	0.95
Capillary number $N_{ca} \equiv \mu U_W/\sigma$	...	15
Porosity of uncompressed substrate	0.5	...
Permeability of uncompressed substrate	3.7×10^{-10} cm^2	3.7×10^{-6}
Minimum clearance of uncompressed substrate in gap between roll	400 μm	4
Effective roll radius	40 cm	1×10^4
Compressibility number $N_{co} \equiv \mu U_W/EH_0^2$	...	1×10^{-4}
Polytropic air compression exponent n	...	1.4

3. Hydrodynamic pressure profile (A), where the unit of distance along the web is H_0, or 0.1 mm, for instance, in the extended base case. Enlargements of (B) the application zone and (C) the metering zone

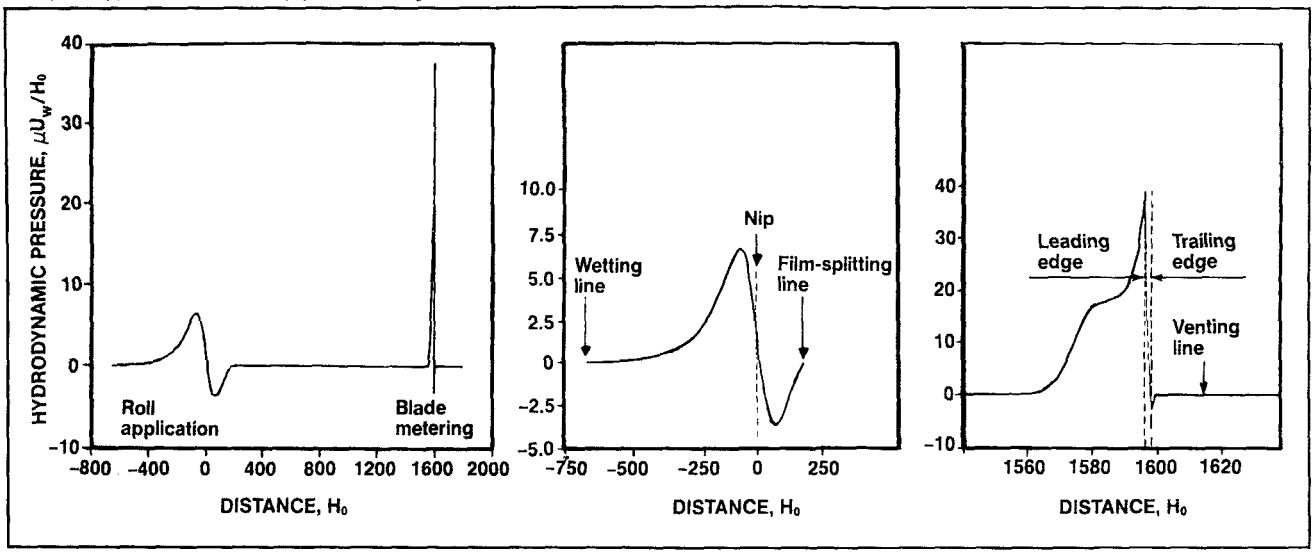

4. The depth of liquid penetration vs. the distance from the application zone nip ($x = 0$) for (A) complete air trapping and (B) no air trapping. The unit of depth is H_0. Further penetration downstream of the venting line is not shown. The curves are for the extended base case (forced and spontaneous penetration together), no capillary pressure (forced alone), and no hydrodynamic pressure (spontaneous alone)

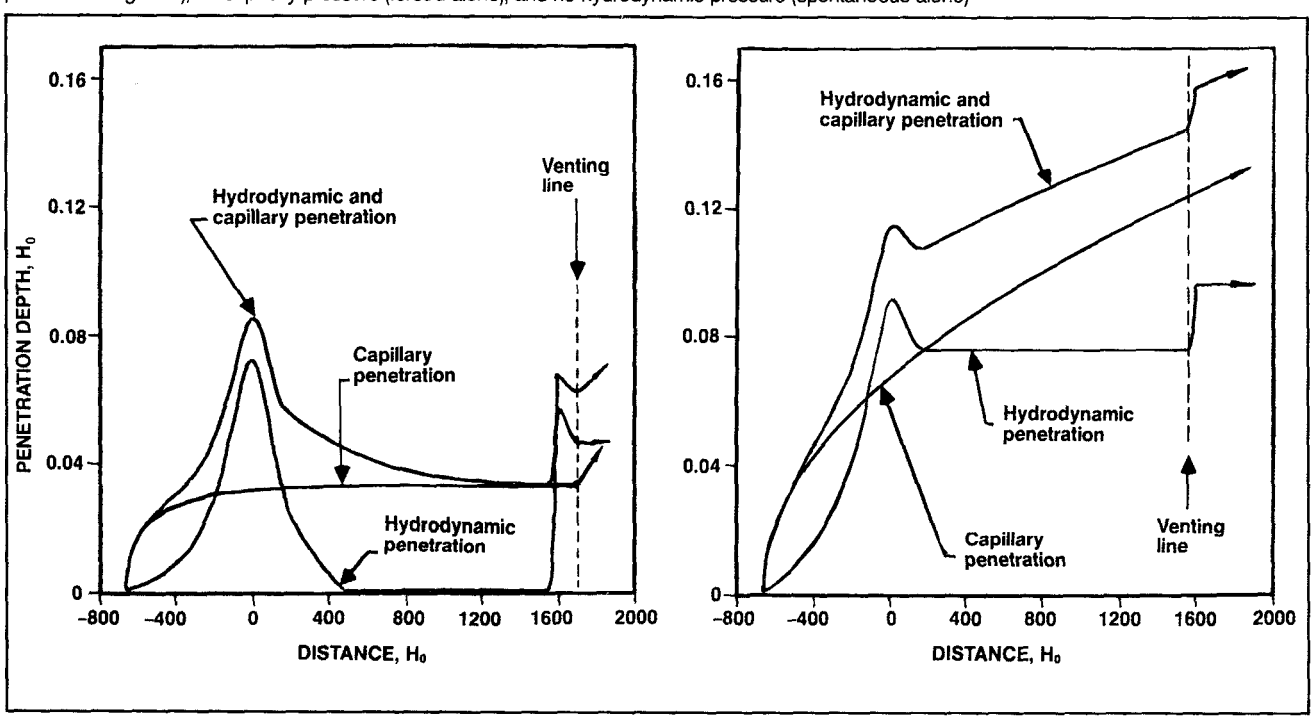

without venting. Thus the location of the venting line, the pressure just upstream of it (or equivalently the fall in pressure at the line), and the coated layer thickness there critically influence the net penetration of liquid at the venting line. The subsequent increment must ultimately be $\Delta Z = t_w(x_v)/\phi_0$, as explained above.

Some earlier models of penetration disregard air trapping and compression. In that extreme, Eq. 12 applies, (that is, $p_G(x) = p_a$), and Eq. 27 indicates that forced penetration would be controlled by the area under the hydrodynamic pressure curve. Indeed, if capillarity-driven, spontaneous imbibition were negligible, liquid would be injected or withdrawn as the hydrodynamic pressure rose above or fell below atmospheric, and the net amount remaining would be proportional to the square root of the area. With capillary pressure active, this amount would be augmented by the spontaneous penetration over the dwell distance $x_v - x_0$, and additionally by $t_w(x_v)/\phi$, from the coated layer.

Illustrative predictions

Extended base case

The utility of the principles organized

into precise form from which predictions can be computed is illustrated by the results presented here. They are for a substrate and a roll applicator characterized by the parameters tabulated above, a transit zone of a particular length, and a bevelled blade metering element as in the base case (*3*). The totality is referred to here as the "extended base case." The Reynolds number (substrate speed times liquid density times substrate thickness divided by liquid viscosity) is 36. The capillary number (substrate speed times acceleration of gravity times the square of substrate thickness divided by viscosity times substrate thickness) is negligible, at 4×10^{-5}.

One set of dimensional quantities to which these parameters correspond is shown in **Table II**. The permeability value is representative, though perhaps on the low side of a wide range over grades (*18, 25, 26*). The value of capillary pressure chosen is representative of a mean meniscus radius of about 14μm, which is probably on the high side for paper.

Under these conditions, in the roll application zone the liquid flux in the gap at the film split is 3.09, of which 2.84 (e.g., a film thickness of 284μm) leaves in the layer carried away by the substrate. (All fluxes are measured in units of U_wH_0). The flux of liquid that has already penetrated the substrate is 0.029. If liquid could not penetrate the substrate, the flux of liquid would be 3.12, of which 2.86 would leave in the layer carried away by the substrate according to a simpler analysis (*21*). Thus, in this case, the flux changes by only 1% along the gap and the simpler analysis would be adequate. The maximum compression of the substrate is only 0.06%, occurring just upstream of the nip; this is insignificant but under other conditions, there can be appreciable compression, as the companion paper indicates (*3*).

Figure 3A shows the pressure profile along the substrate surface over the entire dwell length; Figs. 3B and 3C are enlargements. The maximum in the metering zone (38, e.g., 2.8 atm) is about 6 times that in the application zone (6, e.g., 0.44 atm), reflecting the narrower clearance under the blade for the parameters of this case. The region of elevated pressure in the blade zone is only about 1/20 as long (39, e.g., 2.6×10^{-4}s) as in the applicator zone (667, e.g., 4.4×10^{-3}s). This is followed by a much shorter region of depressed pressure (1.6 vs. 170, or 1.1×10^{-5}s vs. 1.1×10^{-3}s), which terminates abruptly at the venting line. However, what is most important is neither the pressure levels nor the dwell distances or dwell times, but the integral of the pressure profile with respect to distance or, equivalently, time.

Figure 4 shows the depth of liquid penetration into the substrate vs. dwell distance in the limiting cases of (A) complete air trapping and (B) no air trapping. One curve is for the parameters of the extended base case, the second is for the same parameters except that capillary pressure is set to zero, and the third is for spontaneous imbibition by capillary pressure alone. These curves show the relative importance of forced and spontaneous penetration. What is remarkable is the relatively deep penetration up to the nip in the application zone, followed by the delayed expulsion of penetrated liquid as the gas compressed behind it re-expands, the rate of re-expansion being controlled by the Darcy flow resistance to liquid expulsion. The transit zone is just long enough that equilibrium is approached. The pressure of the trapped air falls to almost the capillary pressure (absolute pressure $p_c + p_a$), and liquid leaves until the penetration depth is only slightly more than Z_{eq} (defined above).

But then the abrupt climb of hydrodynamic pressure as the leading edge of the bevelled blade is approached drives liquid back into the pore space, and the trapped air is partially recompressed. After peaking, the hydrodynamic pressure falls precipitously (Fig. 3). Once it drops below the liquid pressure at the menisci ($p_G(x) - p_c$), there again is delayed expulsion of penetrated liquid as the air once more re-expands.

Then the sudden venting of the trapped air decompresses it to atmospheric pressure. Expulsion of liquid ceases, and capillarity-driven, spontaneous imbibition takes over, drawing into the pore space liquid from the layer left coated on the surface of the substrate. The layer thickness is 0.081 (e.g., 8.1 μm), which is 56% of the gap between the substrate and the trailing edge of the blade. The final penetration depth (that is, when all liquid is absorbed into the web by capillary action) in the extended base case is $Z = 0.22$; it is 99% of this at $x = 5700$ (e.g., 57 cm, or 38 ms) downstream in the take-away zone.

5. The pressure profile of air trapped in the pore space of the substrate (units as in Fig. 4)

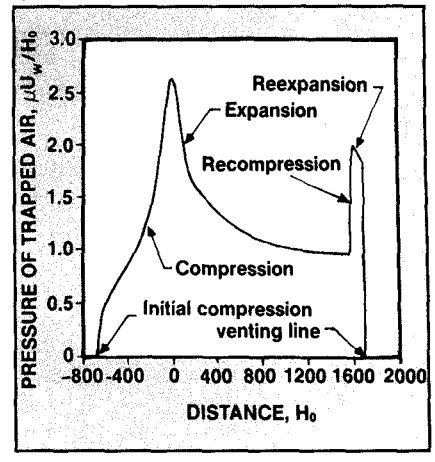

The total liquid flux downstream of the blade is 0.11. Comparison with the total flux in the pore space and the coated layer at the film-split of the application zone reveals that about 96% of the incoming liquid to the metering zone is rejected by the bevelled blade metering element in this extended base case. If the liquid density were 1200 kg/m^3, the wet weight of coating would be 13.4 g/m^2, of which 3.7 g/m^2 would already be in the substrate at the venting line.

Air compression

The hidden actor is the trapped air. Its pressure profile in the limiting case of complete air trapping is plotted in **Fig. 5**, which shows that in the application zone, the air is compressed to almost half of the maximum hydrodynamic pressure there (2.63 vs. 6.0). In the transit zone, it re-expands nearly to the capillary pressure of 0.95. In the metering zone, it is abruptly recompressed, but only to about 1/20 of the maximum hydrodynamic pressure there (2 vs. 38). The air is not even recompressed to the pressure it reaches in the application zone, because the dwell time, or the dwell distance, of approach to the leading edge of the bevelled blade is far briefer. The rate of re-expansion that follows is controlled by the rate of liquid expulsion, which is slow for the reasons mentioned. Finally, the air pressure drops to atmospheric

pressure at the venting line.

The critical role of air compression is even more evident in Fig. 4B, which shows the limiting case in which the underside of the web is somehow vented everywhere to atmospheric pressure. In other words, there is no air trapping. Forced penetration when hydrodynamic pressure exceeds atmospheric, forced withdrawal when it falls below atmospheric pressure, and spontaneous penetration continually can all proceed unopposed. What is noteworthy is the greater part played by capillary-driven, spontaneous penetration when no opposing air pressure builds up. Most significantly, liquid continues to invade in the transit zone (though at a continually diminishing rate, as predicted by the Lucas-Washburn-type formula). In Fig. 4B, the curve for forced and spontaneous penetration together reveals that without air compression, the penetration depth at the position of the venting line would be about 1.5 times greater than in the extended base case, whereas capillarity is responsible for half of the total when air is trapped in the pore space.

In actuality, air arriving in the pore space may be neither completely trapped nor everywhere vented. Moreover, it can flow within the pore space in response to any pressure gradient that is applied to it (as described by Eqs. 8-11). If there is partial venting or other means of air movement, the situation is intermediate between the extremes pictured in Figs. 4A and 4B.

Dwell time

The effect of shortening the transit zone and thereby cutting the dwell time is brought out by **Fig. 6**. When air is completely trapped in the pore space, the dwell time, or dwell distance, has virtually no effect on the final penetration depth. This holds until the distance is short enough that the coating's viscous resistance to expanding gas in its exertion to expel penetrating liquid can no longer keep the liquid trapped in the pore spaces. At such a dwell time, equilibrium penetration has not been reached.

In sharp contrast is the situation when air is not trapped. Dwell time or distance has a substantial effect because capillarity-driven, spontaneous imbibition of the liquid layer deposited by the applicator roll is unopposed. When air is not trapped, the limiting state is total uptake of that liquid layer, so that exactly the same capillary pressure is established at the pore openings on the upper surface of the substrate as at the front between liquid and air down inside the substrate (the same type of equilibrium as is approached in the take-away zone).

The model as it stands does not account for absorption of liquid by the matrix itself—i.e., by swelling. This mechanism may depend extensively on dwell time.

The critical role of air compression is illuminated further by **Fig. 7**, which shows the effect of replacing the roll applicator with a fountain feed that deposits the same layer thickness, so that hydrodynamic pressure is eliminated but dwell time is unchanged. Also shown is the effect of eliminating both the roll applicator and the dwell distance, supplying instead the same liquid film by a fountain feed immediately upstream of the bevelled blade metering element, as in a short-dwell-time blade coater. The conclusion is that in the model developed here, when the air is trapped, the application and transit zones are expendable. Nearly the same penetration depth (about 90% compared with the extended base case) can be achieved with a short-dwell-time configuration that uses the same blade. (This means nearly the same coating thickness and, hence, nearly the same total liquid deposited. However, liquid absorption by the swellable matrix is not accounted for in this model.) However, when no air is trapped, the dwell time in the transit zone is quite important, and the pressure impulse in the application zone significantly affects penetration depth.

Metering gap

Compared to the total penetration in the extended base case, the incremental penetration in the metering zone is minor if air is not trapped in the pore space; on the other hand, it is around 40% of the total if air is trapped. In either event, enlarging the gap seven-fold (by lessening the blade loading) has little effect, because the integrated pressure force on the liquid in the metering zone scarcely changes, although the pressure profile does (Fig. 3).

The main effect of the metering gap is on the coated layer that it delivers. As blade loading is lowered from that of the extended base case, the layer thickness rises in nearly inverse proportion, so there is a major effect on the wet weight of the coating. Conversely, as blade loading is raised, the layer thickness tends to fall, but the relationship is complicated by deformation of the substrate (*3*). In any case, the importance of penetration on coating weight can be expected to increase as the blade is loaded more heavily.

Discussion

The significance of this study is twofold. First, it further indicates how temporary engineering science can be brought to bear in the modeling of complicated coating processes (*2- 4*). (The model under development, however, is far from complete.) Second, it indicates that air can be important when coated liquid penetrates into a porous substrate (*1, 2*). Just how important depends on circumstances that are not yet clear.

Study of the extended base case and a few variations on it illustrates how known physical principles of liquid coating, fluid flow in porous media, and gas compression can be transcribed into equation form, from which predictions can systematically be computed and compared. The predictions can be used to evaluate the relative importance of mechanisms as functions of parameters and trends as parameters change. These are qualitative outputs that help advance the understanding of paper coating processes in terms of basic principles. To yield quantitatively accurate predictions useful in design and operation, all of the principles actually at work must be represented adequately in the equation set, and all of the important parameters must be known well enough. However complete the equation set is and however well known the parameters are, they constitute a model of the process. Such a model can be tested and improved. That is a goal at which this study is aimed.

There are many more variations of the extended base case to be explored under the present model so that it can be tested well. But there are additional physical and physicochemical mechanisms that need to be incorpo-

6. The effect of transit zone length, or dwell distance, on liquid penetration depth. (A) Extended base case (L = 2500) and variation (L = 1800, 1200). (B) When no air is trapped

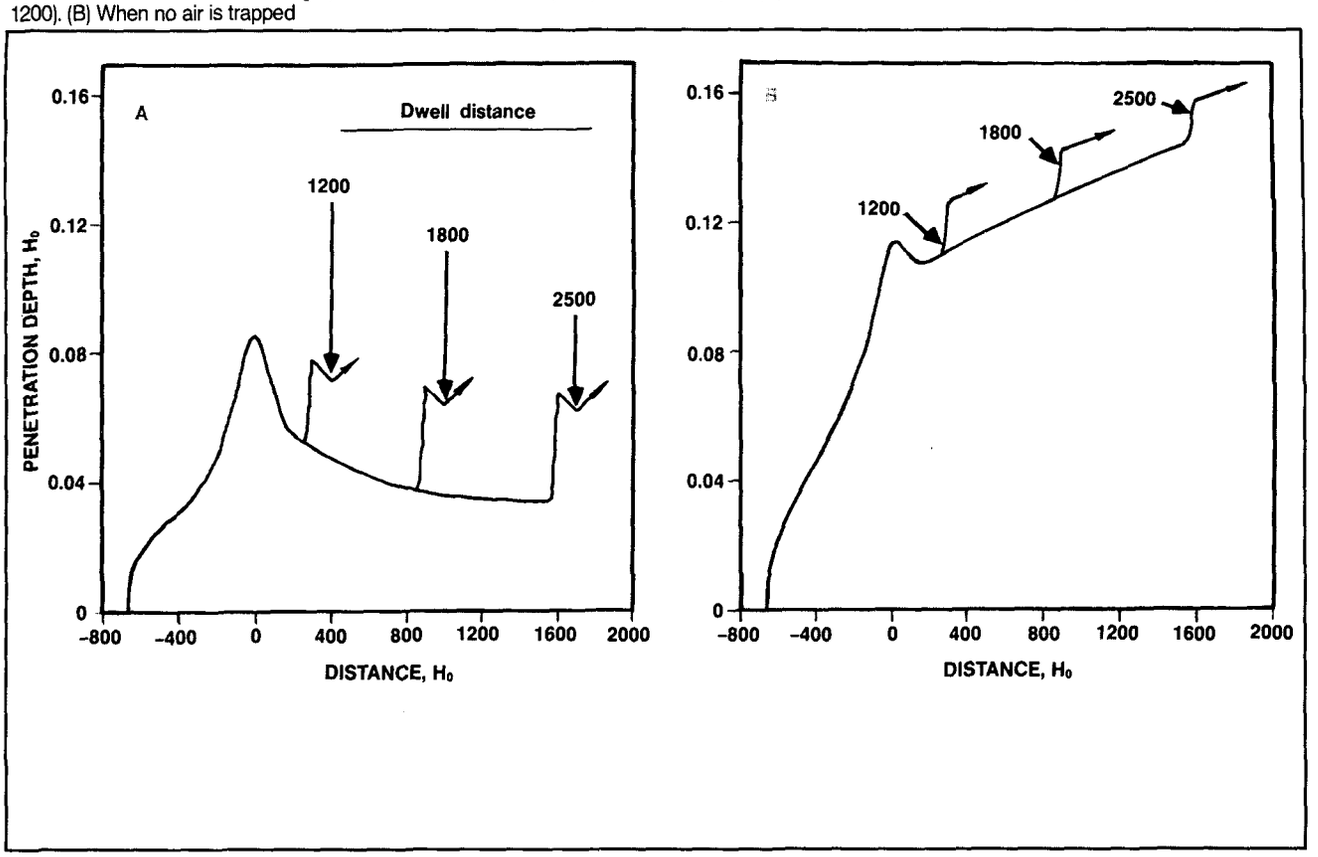

7. The effects of replacing the roll applicator by fountain feed and eliminating the transit zone, to leave a short dwell time blade coater (A) when air is trapped and (B) when no air is trapped

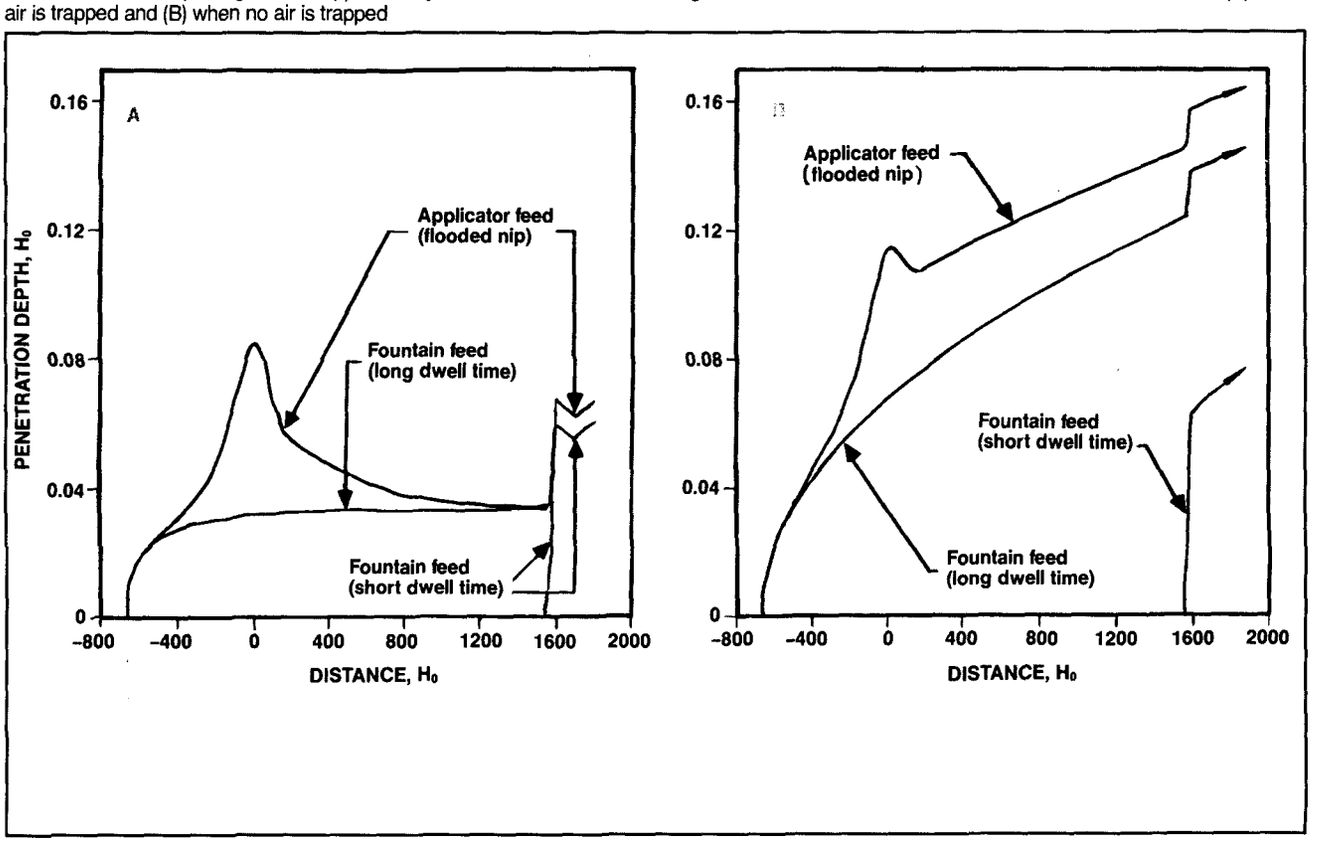

rated in it—and that will further complicate it, making the computation of predictions more formidable. Those mechanisms are discussed elsewhere (*24*).

Each mechanism, once its basic principles are identified and transcribed into equation form, can be incorporated. By computing predictions from the augmented model, which requires an investment in modern large-scale scientific computation, the effects of the mechanisms and their interactions can be explored and evaluated. In this way, we can advance the understanding of the complex interplay of deformable blade, liquid suspension, resident air, elastic backup roll, and the complicated physics of liquid penetration into compressible porous substrates. Sustained effort can bring efficient means of more accurate modeling of blade coating processes and other coating and pressing processes, for the purposes of troubleshooting, design, and optimization.□

Literature cited

1. Eklund, D. and Salminen, P., APPITA 40(5): 340(1987).
2. Saita, F. A. and Scriven, L. E., 1985 Coating Conference Proceedings, TAPPI PRESS, Atlanta, p. 13.
3. Pranckh, F. R. and Scriven, L. E., Tappi J. 73(1): 163(1990).
4. Coyle, D. J., Macosko, C. W., and Scriven, L. E., 1985 Coating Conference Proceedings, TAPPI PRESS, Atlanta, p. 161.
5. Windle, W. and Beazley, K. M., Tappi 50(1): 7(1967).
6. Beisswanger, R. and Sollinger, H. P., 1984 Coating Conference Proceedings, TAPPI PRESS, Atlanta, p. 77.
7. Skowronski, J. and Lepoutre, P., 1985 Coating Conference Proceedings, TAPPI PRESS, Atlanta, p. 41.
8. Sommer, H., 1985 Coating Conference Proceedings, TAPPI PRESS, Atlanta, p. 23.
9. Eklund, D. and Salminen, P., Tappi J. 69(9): 116(1986).
10. Sandas, P. S. and Salminen, P. J., 1987 Coating Conference Proceedings, TAPPI PRESS, Atlanta, p. 97.
11. Nakazawa, T., Morita, H., and Booth, G. L., 1987 Coating Conference Proceedings, TAPPI PRESS, Atlanta, p. 141.
12. Salminen, P. J., Tappi J. 71(9): 195(1988).
13. Tayler, A. B., Q. J. Mech. Appl. Mech. 31: 481(1978).
14. Mohanty, K. K., Davis, H. T., and Scriven, L. E., Surface Phenomena in Enhanced Oil Recovery (Shah, D. O., Ed.), Plenum Publishing Corp., New York, 1981, p. 595.
15. Mohanty, K. K., Davis, H. T., and Scriven, L. E., Soc. Petr. Eng. J., 27: 113(1987).
16. Collins, R. E., Flow of Fluids Through Porous Media, Reinhold, New York, 1961.
17. Dullien, F. A. L., Porous Media, Academic Press, New York, 1979.
18. Knauf, G. H. and Doshi, M. R., 1986 International Process and Materials Quality Evaluation Conference Proceedings, TAPPI PRESS, Atlanta, p. 233.
19. Jaeger, J. C. and Cook, N. G. W., Fundamentals of Rock Mechanics, 3rd edn., Chapman & Hall, London, 1979.
20. Teletzke, G. F., Scriven, L. E., and Davis, H. T., Chem. Eng. Commun. 55: 41(1988).
21. Coyle, D. J., Macosko, C. W., and Scriven, L. E., J. Fluid Mech. 171: 183(1986).
22. Chen, K. S. A. The Fluid Mechanics of Impregnation in Forward Roll Coating, MS Thesis, University of California, Davis, 1986.
23. Cameron, A., Basic Lubrication Theory, 2nd edn., Wiley, New York, 1976.
24. Chen, K. S. A. and Scriven, L. E., 1989 Coating Conference Proceedings, TAPPI PRESS, Atlanta, p. 93.
25. Jackson, G. W. and James, D. F., Canadian J. Chem. Eng. 64: 364(1986).
26. Lindsay, J., Technical Paper Series No. 298, Institute of Paper Chemistry, Appleton, Wis., 1988.

This research was supported by grants-in-aid from Westvaco Corp. and James River Graphics and by grants for computation from the Minnesota Supercomputer Institute. Ferdinand R. Pranckh provided the Metering zone model and useful commentary. The approach was stimulated by discussions with Stephen C. Smith and others of Westvaco, Brian G. Higgins then of the Institute of Paper Chemistry, and various industrial cooperators with the Coating Flows Research Group.

Received for review May 15, 1989.

Accepted Aug. 9, 1989.

Presented at the TAPPI 1989 Coating Conference.